Journal of
Ceramic Science
and Technology

J. Ceram. Sci. Tech., **05** [04] 261-268 (2014)
DOI: 10.4416/JCST2014-00044
available online at: http://www.ceramic-science.com

Additive Manufacturing: Controllable Fabrication for Integrated Micro and Macro Structures

X. Tian*, D. Li, B. Lu

State Key Laboratory for Manufacturing Systems Engineering, Xi'an Jiaotong University
received October 13, 2014; received in revised form November 14, 2014; accepted November 17, 2014

Abstract

Additive manufacturing technology has been developed at Xi'an Jiaotong University for almost twenty years. Innovative process development and frontier application for additive manufacturing technologies have been conducted here since then. In the present paper, the newly developed processes, such as low-cost UV-LED and high-efficiency stereolithography, ceramic stereolithography, and direct metal forming, will be briefly reviewed. Some results of the frontier application research, such as indirect fabrication of ceramic casting molds, wind-tunnel-testing models, and photonic crystals and metamaterials, will be also discussed. On the basis of all these R&D activities, an academic viewpoint on additive manufacturing technologies with "controllable fabrication for integrated micro and macro structures" was proposed and used to guide the further research.

Keywords: Additive manufacturing, rapid prototyping, stereolithography

I. Introduction

Additive manufacturing, also called 3D printing, is a new method to fabricate parts by adding materials layer by layer. This constitutes a bottom-up fabrication process in contrast to the traditional subtractive processes. Any complicated components can be rapidly and precisely fabricated on one single 3D printing machine without any tools or fixtures. Micro and macro structures can be integrally fabricated by means of the 3D printing process owing to the characteristics of the point-surface-volume forming process. Moreover, the texture and structure can be further integrally fabricated, which means that complicated multimaterial textures and contour structures can be synchronously fabricated during the 3D printing process. *Times* magazine listed additive manufacturing as one of the ten fastest-promoted industries in America. *Economist* magazine in England proposed that additive manufacturing will push the realization of the "third industrial revolution" together with other digital fabrication patterns. At Xi'an Jiaotong University, research on additive manufacturing technologies was conducted in the early 1990s. The process principle, materials, and equipment for stereolithography were researched and developed, and a rapid fabrication system was further established in the lab. Based on all these research activities, an active additive manufacturing research group gradually came into being at Xi'an Jiaotong University.

The research group put forward an academic viewpoint for "controllable fabrication of integrated micro and macro structures" according to the characteristics of additive manufacturing process – point-by-point controllable deposition. Components with controllable shape and performance have been fabricated by merging cold and thermal state fabrication methods utilizing polymer, metal, ceramic and composite as raw material. Scientific laws behind the additive manufacturing process from point to volume have been investigated based on experience from the research of the fundamentals, equipment and typical applications with different materials. Meanwhile, frontier research has been conducted to encourage the interdisciplinary innovation, such as bio-fabrication for tissues and organs, metallic parts with directional crystallization microstructure, and ceramic photonic crystals.

In this paper, we should like to briefly review our recent R&D activities on process innovation and frontier research for additive manufacturing technologies.

II. Process Innovation

(1) Low-cost stereolithography with the use of UV-LED light

In order to cut the cost of conventional stereolithography equipment, an LED-SL system with high-power UV-LED light source has been developed. This consists of an LED chip, a focusing lens set, a controllable LED power supply, an X-Y workbench, a Z-axis elevator and the manipulation software as shown in Fig. 1 [1]. The divergent UV light emitted from the LED is focused on the resin surface by the focusing lens set. The workbench drives the lens set to scan along X-Y plane controlled by the software system. In comparison with UV lasers, the price and energy consumption of LEDs are much lower, which conforms to the concept of Green Manufacturing. With the growing demands for inexpensive SL apparatus, a broad potential application can be anticipated. There is, however, still a technical problem that needs to be solved. The focusing lens set is a little heavy. With the increase of the scanning speed, vibration of the lens set has an obvious effect on the scanning accuracy. To raise the scanning speed and reduce

* Corresponding author: leoxyt@mail.xjtu.edu.cn

vibration, a light optical device is required to substitute the spherical lens.

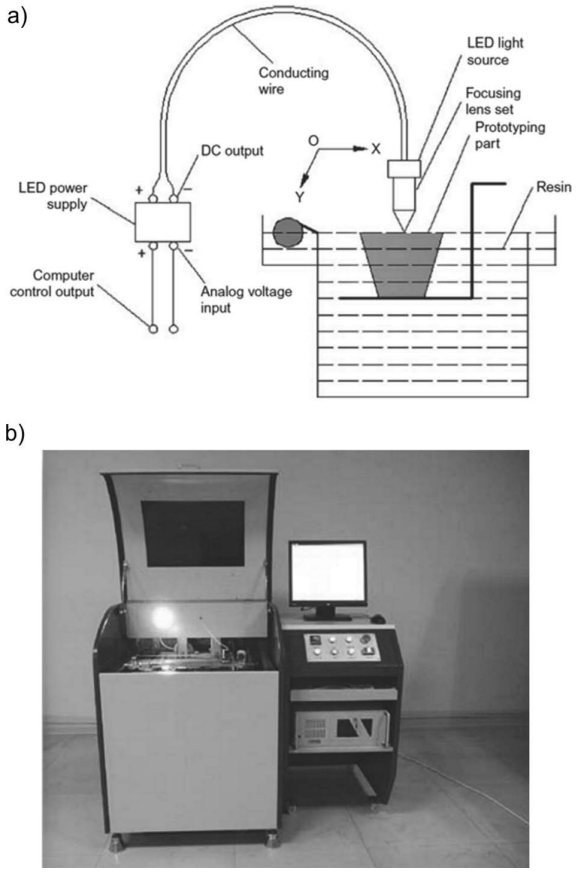

Fig. 1: Schematic showing the LED-SL process (a), and the machine developed by Shaanxi Hengtong Intelligent machine Co., Ltd (b).

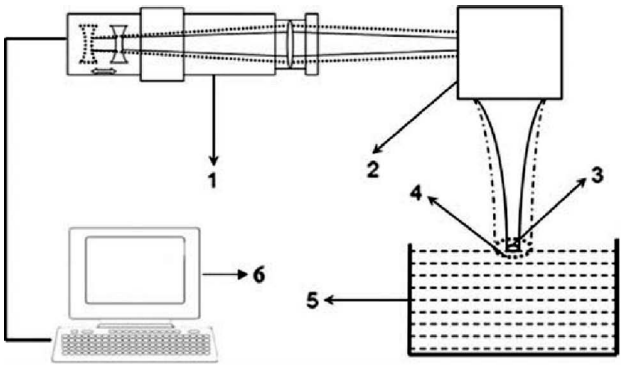

Notes: 1– dynamics focusing mirror; 2 – laser beam before adjusting dynamics focusing mirror; 3 – laser beam after adjusting dynamics focusing mirror; 4 – laser beam spot after adjusting dynamics focusing mirror

Fig. 2: Variable laser beam spot size with dynamic focusing lens.

(2) High-efficiency stereolithography

A new strategy to improve the efficiency of the stereolithography (SL) process has been developed by using a dynamic focusing lens to control the beam spot size on the liquid surface. During the process, the overall focal length of the optical system is changed by the diverging optics moving along the optical axis in the dynamic focusing unit, synchronized with the mirror motion in the scanner head, as shown in Fig. 2. When the beam spot on the resin surface varies with the focus length, the laser power is also adjusted synchronously to maintain a constant laser energy density. Otherwise, the curing depth was decreased and the curing width was increased when the laser spot size was enlarged under the condition that laser power remained unchanged. The microstructures of cross-sections in the curved single lines are shown in Fig. 3. Meanwhile, the laser spot compensation mechanism has been optimized for the variable laser spot size process in order to obtain the same fabrication accuracy as with the traditional SL process. The variable beam spot process was able to improve the building efficiency by 30 percent without increasing the cost of system, while maintaining the same accuracy as with the conventional SL process [2].

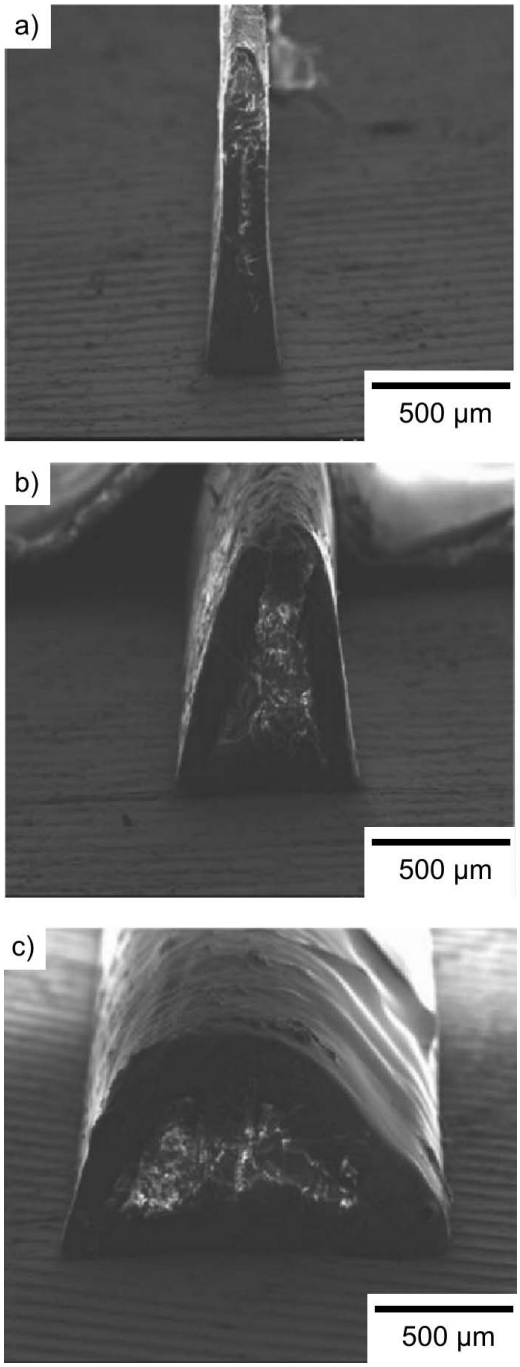

Fig. 3: SEM images of the cross-section of cured single line with laser beam spot size a) 0.8 mm, b) 0.16 mm, and c) 0.36 mm, respectively.

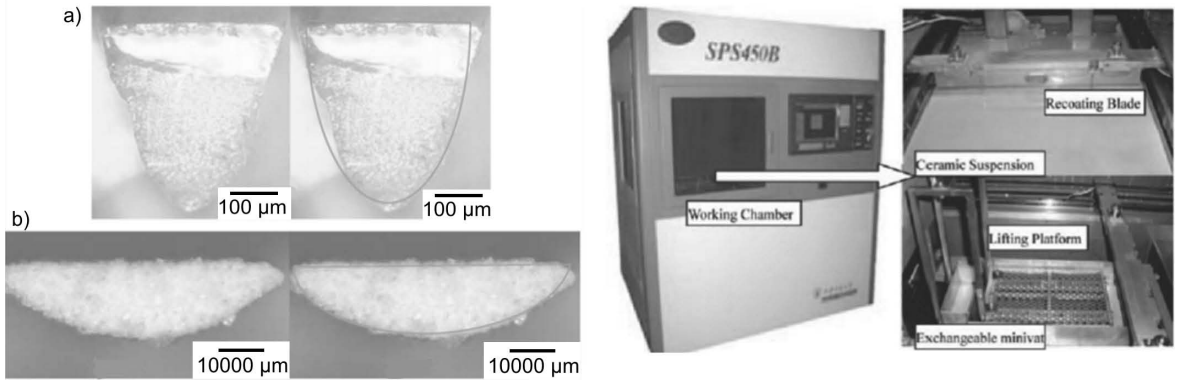

Fig. 4: Comparison in the profiles with photosensitive resin and ceramic suspension (a), and the developed CSL machine.

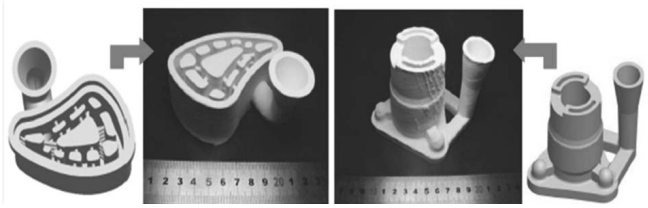

Fig. 5: Ceramic casting moulds fabricated with the CSL process.

(3) Ceramic slurry Stereolithography (CSL)

To extend the application fields for the stereolithography process, UV-laser-curable ceramic slurry was prepared for the direct fabrication of ceramic components. The influence of the silica suspension ingredients and laser exposure on the curing behavior of the highly concentrated aqueous silica suspensions was investigated [3,4]. The curing behavior of aqueous ceramic suspensions was studied by analyzing the profiles of the single cured lines in comparison with that of the photosensitive resin, as shown in Fig. 4a. The magnified photographs of the cross-sections of a single cured line in this silica suspension were compared with that of a conventional resin (Somos 14120, DSM Somos, USA). In the case of the resin, it has a depth of 400 mm and a width of 360 mm, which is smaller than its depth. In comparison, the dimensions of the ceramic suspension in this study are about 190 mm deep and 680 mm wide, flattened by attenuation of the forward laser energy by ceramic filler and widened by lateral scattering. These phenomena reveal that the cured line width and depth are governed by lateral scattering and energy absorption of the ceramic respectively. Experimental results showed that the cured depth and width of single cured lines increased with the ceramic mean diameter and monomer concentrations. The cured width of single cured lines decreased with the solid content, but the cured depth increased with the solid content of silica suspensions. The cured depth and width of the single cured line all decreased with the laser scanning speed. The experimental results show that the ingredients of ceramic suspensions and laser exposure all have a considerable influence on the curing behavior of the highly concentrated silica suspensions, which indicates that the formula is an intrinsic factor for the curing behavior of ceramic suspensions while laser exposure is an exterior factor. A ceramic stereolithography machine was developed on the basis of the SPS 450B UV-laser stereolithography machine, as shown in Fig. 4b. Ceramic parts, such as ceramic casting moulds, were fabricated with this CSL process, as shown in Fig. 5.

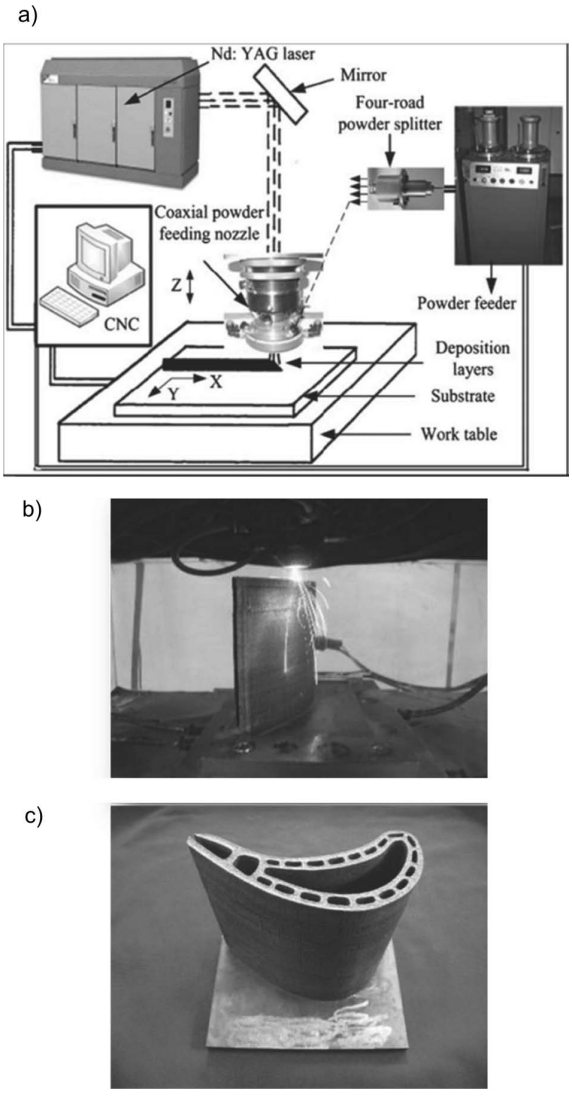

Fig. 6: Schematic showing the direct metal forming process (a), the laser cladding process (b), and the fabricated turbine blade (c).

(4) Direct metal forming

A schematic showing the direct metal forming system is shown in Fig. 6a [5,6]. It primarily includes a 1000W Nd:YAG laser, a powder feeder, and a coaxial powder

feeding nozzle. In the laser cladding process, the metal powder layer being deposited was simultaneously irradiated by a laser beam with a focused diameter of 0.5 mm. The stream field of powders was defocused on the depositing surface with a focused spot about 1 mm below the depositing layer. The N_2 feeding rate was 8 l/min. AISI316L powders with a diameter of 50–100 nm were used in the experiments, and the substrate was of the same material. Experimental results showed that the metal powder stream and laser specific energy are both important factors that control the high-temperature behavior of the molten pool and determine the microstructure of the laser scanning track. Based on the optimized processing conditions, a high-definition steam turbine blade of 316L was fabricated. The surface quality of the fabricated blade was measured, and surface roughness (Ra) was in the range of 10.08 to 26.51 micrometers, as shown in Fig. 6c. A controllable cooling approach was employed in the developed equipment to achieve the required temperature gradient by means of controlled jetting of liquid argon on the forming samples, as shown in Fig. 7. Microstructures of fish-scale type are obtained easily because the molten pool cools quickly with the natural cooling method, but fine columnar crystals can be achieved on the non-columnar-crystal substrate of 316L with the intermittent liquid argon cooling method, as shown in Fig. 8.

III. Application Research

(1) Indirect fabrication of ceramic casting mould

A new manufacturing process for an integral ceramic mould was proposed based on the combination of the gel-casting process with SL technology [7,8]. The basic steps in the fabrication process for the integral ceramic mould are shown in Fig. 9. First, a process system was designed and its corresponding prototype was rapidly fabricated by means of SL. Ceramic slurry was then poured into the prototype mold in a gel-casting process. The slurry was polymerized *in-situ* to form a green gel ceramic body, of which all the parts were connected to form an integral component. Finally, the integral ceramic mold was obtained by means of vacuum drying, pyrolyzing, and sintering. Fig. 10 shows the prototype of a hollow blade and the metal parts fabricated by casting metal into the ceramic mold prepared according to the process described above.

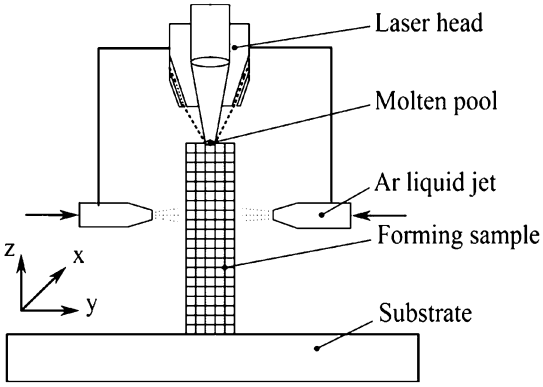

Fig. 7: Schematic showing the controllable cooling approach with the use of liquid argon.

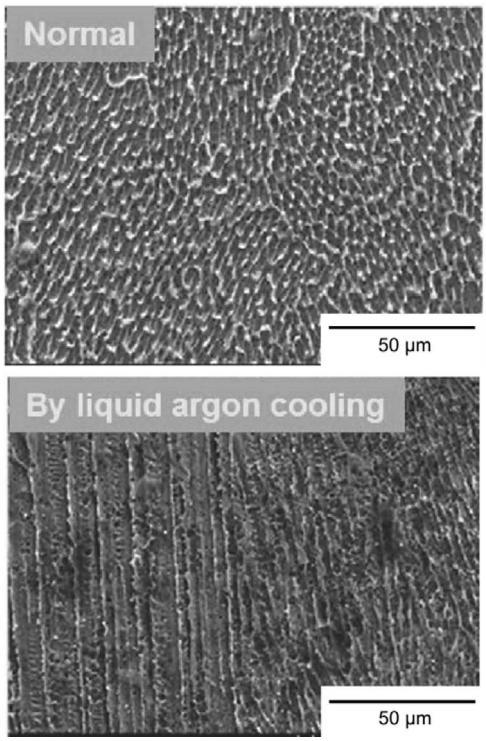

Fig. 8: Microstructures of the samples fabricated with the application of normal natural cooling and liquid argon cooling, respectively.

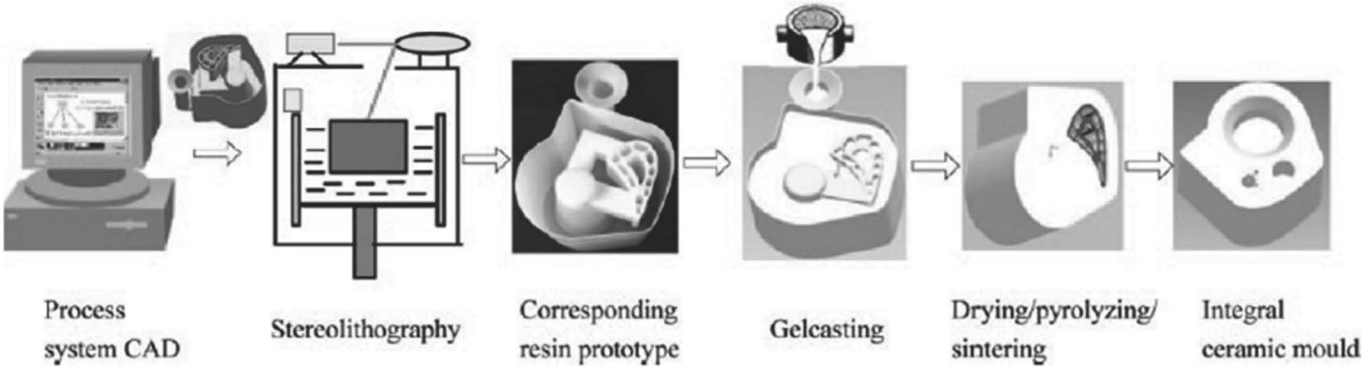

Fig. 9: Basic principles of the integral ceramic mould manufacturing process.

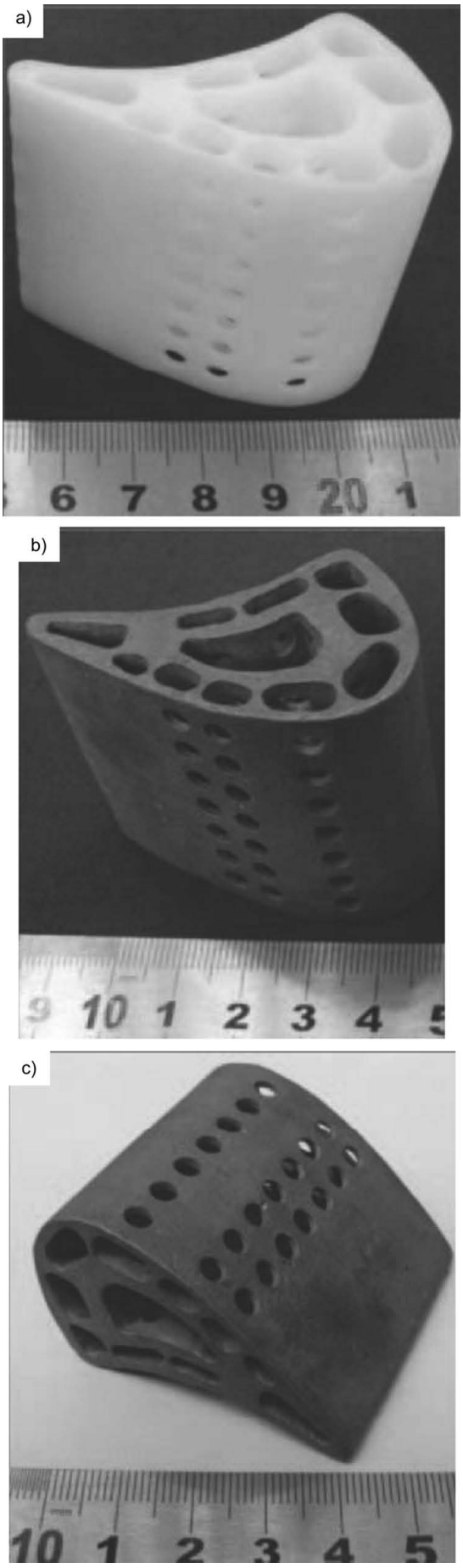

Fig. 10: The SL prototype of a hollow blade (a), metal blade cast with the use of the ceramic mould, front view (b), and side view

(2) Wind-tunnel testing (WWT) models

Based on rapid prototyping, a rapid fabrication technique for wind-tunnel models of flight vehicles has been put forward. An integral tap-passage pressure model was developed, derived from the study of dimensional compensation, tap and passage design and passage configuration design [9]. Focusing on the design and fabrication of structure-similar aeroelastic models, a new method is presented in the paper and validated with the modal test. A new metal-resin composite structure for the wind-tunnel models was fabricated with a combination of SL and electrochemical deposition. Time and cost can be cut with the application of this new technology. The speed of development for the new design of vehicles can be improved dramatically.

The fabrication process includes the following steps. First, the plastic prototypes were fabricated by means of the stereolithography process with photosensitive resin, as shown in Fig. 11a. Chemical treatment was employed to roughen the surface in order to ensure sufficient adhesion of the deposited metal on the SL resin. Prior to the electrodeposition process, the SL part surface must be made conductive. For this, electroless deposition is chosen because it provides a better bond than carbon painting. It is done in an electroless nickel deposition bath, wherein a 1–2-μm-thick layer of nickel can be deposited. After nickel electrodeposition (Fig. 11b) and assembly, the parts were tested in the wind tunnel.

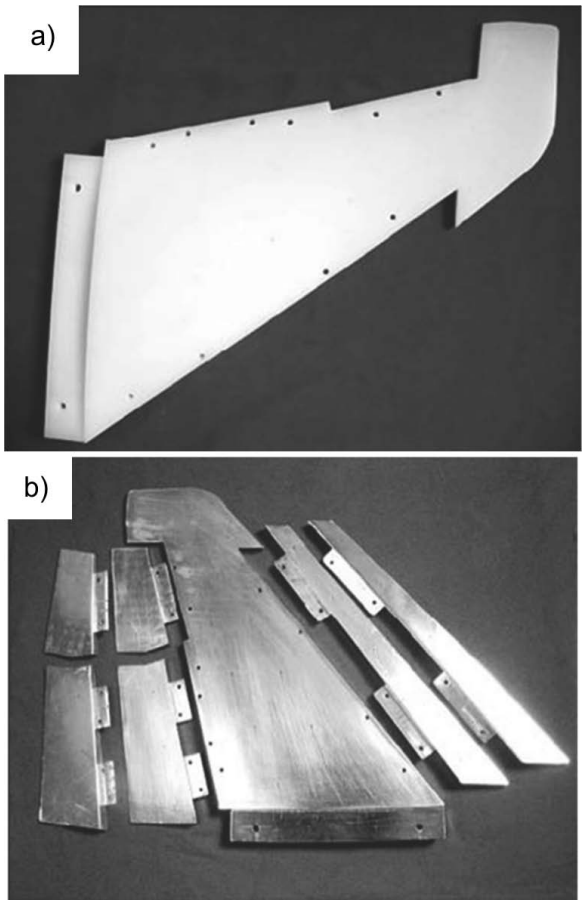

Fig. 11: Surface pressure SL model of main airfoil (a), components of the pressure model with three pairs of deflecting control surfaces (b).

(3) Photonic crystal and metamaterials

(a) *Photonic crystal (PC)*

Two different fabrication processes, direct ceramic stereolithography as described in Section II.(3) and the indirect process (discussed in Section III.(1)), were applied to prepare ceramic photonic crystals. Ceramic PC structures fabricated with the CSL process are shown in Fig. 12a. For the indirect process, the SL process was combined with gel-casting to fabricate 3D PCs (GHz) with diamond structures. An epoxy resin mold of the inverse diamond PC structure was produced by means of the SL process with a lattice constant of 12 mm. Then, the gel-casting method was applied to cast the alumina slurry containing 55 vol% Al_2O_3 powder into the resin mold in order to obtain the whole PC structure. The high refractive index contrast between the lattice and matrix is required in order to get a larger PC band-gap. So the sample was put through a sintering process to increase the dielectric constant of the ceramic part. The fabricated ceramic photonic crystal is shown in the inset of Fig. 12b. The band gap of such a 3D PC structure was measured, as shown in Fig. 12b. Owing to the complete band gap in three directions, 3D PC structures can be used in waveguides and substrates for the microwave antenna [10].

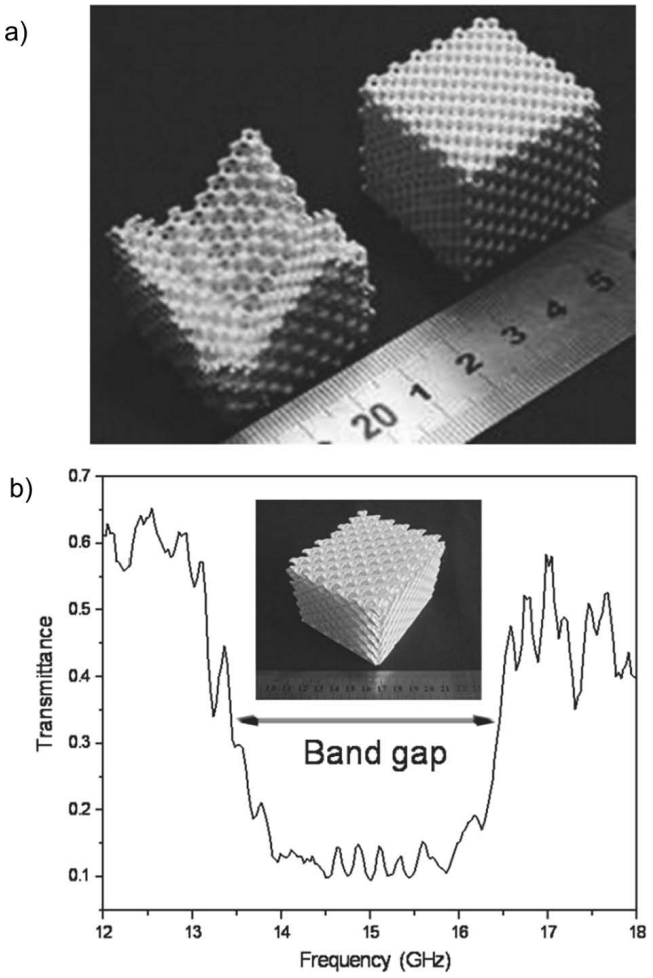

Fig. 12: Photonic crystals fabricated with ceramic stereolithography (a), indirect ceramic component fabrication process (b).

(b) *Metamaterials*

A free-space broadband carpet-cloak, designed by means of transformations optics and quasi-conformal mapping, was realized with all-dielectric gradient index rod-connected diamond-structured photonic crystals (PCs) in a metamaterial regime [11]. A complex three-dimensional sample with smooth continuous changing unit cells was fabricated precisely with stereolithography (SL) using photo-curable resin. With the gradual variation of the unit cell constitutive parameters of the diamond-based PCs with nearly isotropic properties, the required complex spatial distribution of the refractive index profile was ideally achieved to reduce the scattering of the electromagnetic wave. The non-resonant property of the sub-wavelength PCs unit cell resulted in broad bandwidth and relatively low loss. The component produced by means of SL is shown in Fig. 13a. The performance of the carpet cloak was simulated, as shown in Fig. 13b. The irregular perturbation caused by the bump resulted in two main lobes in the scattering field, while the cloaked bump and the conducting plane generated a similar single main lobe. The main lobe produced by the cloaked bump was a bit wider, owing to a slight impedance mismatch caused by the removal of the background medium. The simulation result proved that the designed carpet cloak achieved a good performance.

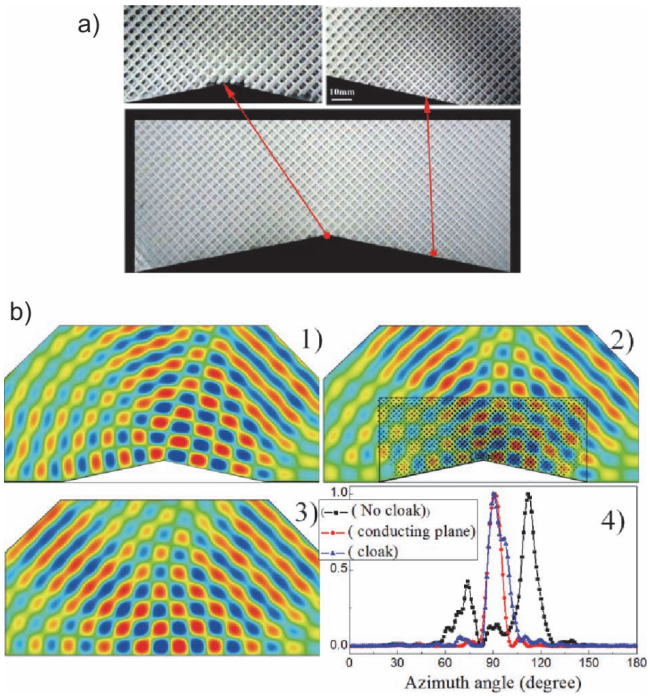

Fig. 13: The fabricated carpet cloak with smooth transition between adjacent unit cells (a), and simulations of the electric field distributions of (1) a bump, (2) a bump concealed by the proposed carpet cloak, and (3) conducting plane. (4) The far-field patterns of the scattered electromagnetic waves for above three cases (b).

V. Conclusions

Based on the current research activities, additive manufacturing technologies will be further developed with focus on the following aspects by the research group at Xi'an

Jiaotong University. First, integral fabrication of the texture and structure will be realized to achieve the controllable fabrication of the parts from the microstructure texture to the macroscopic structure. For example, in the design and fabrication process of the parts with composite materials, inside texture and outside structure can be synchronously finished. Controllable fabrication for integrated micro and macro structures will then be finally achieved. Second, materials used in the additive manufacturing process will be widened further from the traditional resin to metal and ceramics, finally to composites and multimaterials. Finally, intensive interdisciplinary collaboration between physics, chemistry, material, mechanical and control engineering, etc, will be implemented for further innovative process development and application.

References

1 Xie, R., Li, D., Chao, S.: An inexpensive stereolithography technology with high power UV-LED light, *Rapid Prototyping J.*, **17**, [6], 441 – 450, (2011).

2 Cao, Y., Li, D., Wu, J.: Using variable beam spot scanning to improve the efficiency of stereolithography process, *Rapid Prototyping J.*, **19**, [2], 100 – 110, (2013).

3 Zhou, W., Li, D., Chen, Z.: The influence of ingredients of silica suspensions and laser exposure on UV curing behavior of aqueous ceramic suspensions in stereolithography, *Int. J. Adv. Manuf. Tech.*, **52**, 575 – 582, (2011).

4 Chen, Z.: Direct fabrication of ceramic parts based on stereolithography [D]. M.E, thesis. Xi'an: Xi'an Jiaotong University, 2010

5 Lu, Z.L., Li, D.C., Lu, B.H., Zhang, A.F., Zhu, G.X., Pi, G.: The prediction of the building precision in the laser engineered net shaping process using advanced networks, *Opt. Laser. Eng.*, **48**. 519 – 525, (2010).

6 Zhu, G.: Laser metal direct forming process of hollow turbine blades [D]. Ph.D Dissertation. Xi'an: Xi'an Jiaotong University, 2012

7 Wu, H.: A new rapid manufacturing technology of the casting mold with integral ceramic core/shell for hollow turbine blades [D]. Ph.D Dissertation. Xi'an: Xi'an Jiaotong University, 2009

8 Wu, H., Li, D., Tang, Y., Guo, N., Cui, F., Sun, B.: Rapid casting of hollow turbine blades using integral ceramic moulds, *P.I. Mech. Eng. B. J. Eng.*, **223**, 695 – 702, (2009).

9 Zhou, Z., Li, D., Zhang, Z., Zeng, J.: Design and fabrication of a hybrid surface-pressure airfoil model based on rapid prototyping, *Rapid Prototyping J.*, **14**, [1], 57 – 66, (2008).

10 Hu, Y., Li, D., Dai, W., Wang, M., Wang, H., Wu, H.: Fabrication of three-dimensional electromagnetic band-gap structure with alumina based on stereolithography and gel-casting system and its performance study, *J. Manuf. Syst.*, **31**, 22 – 25, (2012).

11 Yin, M., Tian, X.-Y., Han, H.X., Li, D.: Free-space carpet-cloak based on gradient index photonic crystals in metamaterial regime, *Appl. Phys. Lett.*, **100**, 124101, (2012).

12 Li, D., Tian, X., Wang, Y., Lu, B.: Developments of additive manufacturing technology, *Electromachining & Mould*, **269**, 20 – 22, (2012).